

Lehigh University Lehigh Preserve

Eckardt Scholars Projects


Undergraduate scholarship

5-1-2014

Targeting Proteins to Cancer Cell Membranes Using the pH Low Insertion Peptide

Amar Shah
Lehigh University

Follow this and additional works at: <https://preserve.lehigh.edu/undergrad-scholarship-eckardt>

 Part of the [Medical Cell Biology Commons](#), and the [Medicinal and Pharmaceutical Chemistry Commons](#)

Recommended Citation

Shah, Amar, "Targeting Proteins to Cancer Cell Membranes Using the pH Low Insertion Peptide" (2014). *Eckardt Scholars Projects*. 25.
<https://preserve.lehigh.edu/undergrad-scholarship-eckardt/25>

This Article is brought to you for free and open access by the Undergraduate scholarship at Lehigh Preserve. It has been accepted for inclusion in Eckardt Scholars Projects by an authorized administrator of Lehigh Preserve. For more information, please contact preserve@lehigh.edu.

Targeting Proteins to Cancer Cell Membranes Using the pH Low Insertion Peptide

The pH Low Insertion Peptide (pHLIP) is able to unidirectionally insert itself in membranes at low pH, a physiological marker of cancerous cells. Thus, the pHLIP peptide has potential use as a dual targeting and delivery system for cancer therapeutics. We are investigating pHLIP-protein constructs to further our understanding of protein-membrane interactions and pHLIP dynamics in an attempt to target proteins to cancer cell membranes.

Amar Shah
Lehigh University Eckardt Scholars Senior Thesis
Class of 2014

Advisor: Damien Thévenin
Lehigh University
Department of Chemistry

Cancer - An Introduction

Cancer can be broadly defined as the unregulated growth and proliferation of cells. Cancer has an extremely high disease burden and currently is the subject of very active research. Oncogenesis, the birth of a tumor, is usually caused by a failure of normal metabolic and growth-regulating factors in a cell. In a healthy cell, there exists a dynamic interplay between growth-promoting factors (mitogens) and inhibitory signals. Mutations that disrupt this delicate balance, either by generating hyperactive growth signals or preventing anti-proliferative activity of tumor-suppressor genes, often lead to cancer. Typically, such deleterious DNA mutations are rapidly corrected by DNA proofreading machinery; however, mutations or cellular injuries that impair these crucial repair mechanisms can leave individuals suspect to cancerous growths.

Cancer cells may be differentiated from healthy tissue in several regards. Tumor cells typically over-express certain receptors, which are unique to the particular type of cancer. Identifying these receptors is often difficult, as the target proteins are also expressed by other somatic cells. Therefore, determining a threshold of over-expression compared to healthy tissue can be challenging. Even if a majority cells within the tumor may have a given cell-surface proteome, others will not. There is evidence that cancer cells may be capable of evolving in response to environmental factors, changing their cell-surface proteome over time (Tomlinson *et al.*, 1996). Thus, receptor targeting is a prevalent but flawed tumor targeting and identification technique.

Another relatively unique physiological marker of cancerous cells is an acidic external microenvironment, resulting from a highly active metabolic state. Typically, the presence of oxygen inhibits glycolysis in favor of oxidative phosphorylation, an effect known as Pasteur's effect (Gatenby *et al.*, 2004). However, in cancerous tissue, even in ample O₂ supply, rates of

glycolysis are significantly elevated; this "aerobic glycolysis" is referred to as the Warburg effect (Barar and Omid, 2013). This effect is believed to be a response to the intermittent hypoxia experienced in early tumorigenesis, as vascularization may be poor, leading to inadequate oxygen supplies. The increased reliance upon glycolysis results in high levels of lactic acid and requires high levels of glucose uptake, further aiding the Warburg effect (Jang *et al.*, 2013).

The rapid metabolism results in the accumulation of protons and acidic byproducts within the cytoplasm. To maintain a proper internal pH, cancer cells up-regulate proton transporters to shunt protons across the cell membrane, where they accumulate in the local extracellular space. The resulting increase in acidity can drop the pH of the external microenvironment while alkalizing the internal environment. While direct characterization at this external microenvironment has proven to be experimentally difficult, current estimates show a local pH that is likely within a range of 6.0-6.5. Other highly active cells, including those involved in inflammatory responses and immune mobilization, may exhibit similar physiological markers. However, *in vivo* studies have shown minimal off-target tagging of systems capitalizing upon this physiomer of cancerous tissue.

Cancer Therapy

Current cancer therapies, while effective at prolonging the lives of patients, often represent stop-gap solutions; complete tumor recession is rare. The current approaches to treatment are a balancing act between controlling tumor growth and minimizing collateral damage. Each approach has its limitations, and there exists no singular optimal approach to the treatment of cancer. Surgical removal, radiation therapy, and chemotherapy stand as three current pillars of cancer treatment.

Surgical resection, often the preferred method of treatment for complete tumor removal, provides the added benefit of allowing biopsy of surrounding tissue to assess the invasiveness of the tumor. However, surgery may be difficult or impossible in the cases of deep tissue tumors and does not provide a therapeutic benefit against undetected metastases. Additionally, patients may be unfit for surgery due to general illness. Radiation therapy is often used to shrink tumors prior to surgical removal or as a standalone therapy. A limiting constraint is the ability of radiation to be targeted to specific regions of the body to target the tumor while sparing healthy tissue.

Chemotherapy, the use of cytotoxic molecules to kill proliferating cells, is routinely used but causes severe systemic damage. Monoclonal antibody (mAb) therapy, a subset of chemotherapy, currently stands as a frontline therapeutic for cancer patients. mAbs are designed to stimulate an immune response to cancerous cells by selectively targeting particular over-expressed membrane proteins, leading to a more finely tuned strategy for specific cancer types.

While immortalized cell lines may be homogeneous, primary cancer tissue tends to be composed of a variety of cell types. If a few tumor cells remain untargeted, the tumor could simply regenerate post-treatment. Targeting a given receptor with mAbs can also induce a selective pressure upon the tumor tissue, which may then respond via microevolution to avoid the therapeutic (Tomlinson *et al.*, 1996). Therefore, complete eradication of the tumor often requires other adjuvant therapies in addition to the primary treatment. Another key drawback to monoclonal antibodies is the presence of off-target activity. While tumor cells may overexpress a given receptor, it is likely present on a variety of other somatic cell surfaces (Thévenin *et al.*, 2009). Thus, a dose needed for efficacious tumor recession may also significantly impact healthy tissue. In general, chemotherapy tends to have a major cost upon quality of life.

There are several new areas of active research focused upon improving cancer therapeutic delivery and targeting. Drug-loaded lipid vesicles, sometimes tagged with particular targeting proteins, have been used to shuttle drugs into cells. Other approaches have attempted to capitalize upon endocytosis and later endosomal drug release. Recently, two antibody-drug conjugates (brentuximab vedotin and trastuzumab emansine) have been approved for use in human patients (Haddley 2012; LoRusso *et al.*, 2011). These approaches, however, still rely upon biomarkers that are not wholly unique to tumor tissue and may lead to incomplete therapeutic action. Given the heterogeneity of receptor expression in target and off-target cells, a universal marker of cancer would be a preferable target. The use of cell-penetrating peptides and selective membrane translocators are also currently being investigated as delivery vehicles for small-molecule therapeutics (Thévenin *et al.*, 2009).

pHLIP: Discovery, Characterization, and Properties

The study of membrane proteins is integral to elucidating biological function at a molecular and cellular level. Membrane proteins may span the entire bilayer, protrude through one face of the bilayer, or exist in a peripherally associated state. Membrane proteins play a role in a wide variety of cellular functions, including cell-cell recognition, cell adhesion, signal transduction, regulation of ion transport, mediation of endocytosis and exocytosis, enzymatic catalysis, and structural scaffolding.

The first member of the pH-Low-Insertion-Peptide (pHLIP) family was identified via the isolation and characterization of each of the seven transmembrane (TM) helices of bacteriorhodopsin. While six of the seven helices showed properties characteristic of membrane-spanning domains, helix C showed novel properties in aqueous solution (Hunt *et al.*, 1997a). While typical TM domains are highly hydrophobic, helix C showed solubility up to micromolar

concentrations. The pHLIP peptide was derived from this bacteriorhodopsin helix C (Hunt *et al.*, 1997b). pHLIP variants consist of small cytoplasmic and extracellular domains flanking a membrane-spanning TM domain, whose structure is typically highly conserved.

Further characterization led to identification of a pH mediated helical transition in the presence of liposomes. In solution, the pHLIP peptide exists in one of three states. In concentrations in the low micromolar range, the pHLIP peptide exhibits a random coil formation. In the presence of cell membranes (or mimetics, such as liposomes), the pHLIP peptide associates with the phospholipid bilayer in a semi-structured state, an interaction mediated by hydrophobic residues within the TM region. At lower pH, the pHLIP peptide can undergo a helical transition as the C-terminus of the peptide is inserted across the bilayer. This transition is facilitated by protonation (charge neutralization) of key carboxylates within the TM region.

The three states of the pHLIP peptide have been confirmed via biophysical assays: circular dichroism (CD), oriented CD, and Fourier-Transform Infrared (FTIR) Spectroscopies, as well as Tryptophan (Trp) fluorescence assays. CD assays of the pHLIP peptide determined that the random coil state was primarily unstructured and the peripherally-associated state only moderately more structured. However, reduction of pH in the presence of a lipid membrane showed a distinct helical transition in the secondary structure. Follow-up studies monitoring Trp fluorescence showed an increase in intensity following the helical transition and reduced access of the Trp residues to soluble quenchers. These results, taken in conjunction, verified helical insertion into the membrane and ruled out a simple peripheral helical state. Additional studies confirmed the directionality of the insertion; the C-terminus inserts across the membrane while the N-term remains externally present in *all* cases.

The mechanism of pHLIP insertion was quickly elucidated and several functional variants were found. In the TM region of the inserted helix lie two aspartic acid residues, located at positions 14 and 25 (Musial-Siwiek *et al.*, 2010). Upon lowering of pH within the membrane's microenvironment, protonation of the carboxylate sidechain of D25 leads to a semi-helical transition and burrowing of the peptide's C-terminus into the hydrophobic membrane core. Subsequent protonation of D14 facilitates complete helical formation as the TM region inserts fully across the membrane. This process is reversible, as pH increases beyond the $pK_{\text{Insertion}}$ show extraction of the pHLIP peptide from membranes. In native pHLIP, the transition pH has been found to be approximately ~ 6.0 (Reshetnyak *et al.*, 2007). Variants using glutamic acid (E) residues in place of either D14 or D25 show similar properties, with a transition pH in the range of 6.5-7.0 (Barrera *et al.*, 2011). Modification of insertion characteristics has proven difficult, as the pHLIP peptide is relatively intolerant of modifications to key residues within the TM region.

A significant finding related to this pH-dependent membrane insertion was the exergonic nature of the process, the magnitude of which hinted at potential uses of this insertion process. Investigation of this phenomenon led to the discovery of pHLIP-mediated membrane translocation of small molecules (Reshetnyak *et al.*, 2006).

pHLIP has promise as a dual targeting-delivery system for small molecule and peptide theranostics to highly metabolic cells, including tumor cells and cells at the sites of inflammatory response. The pH-dependence of insertion presents a novel mechanism by which these types of tissue can be targeted, without necessitating the use of specific receptors. Since the targeting mechanism is physiological in nature, the use of pHLIP-targeting should be applicable to a wide variety of cancers and inflammatory states, more-so than the standard Ab-mediated targeting systems.

pHLIP can be modified in a variety of ways to incorporate functional ligands, including small molecules and peptides. pHLIP can be genetically engineered to be expressed as a fusion protein construct. Addition of cysteine residues at either terminus can facilitate thiol-mediated linkage. If translocated into the cytosol, reducing conditions release the disulfide-linked drug. Traceless linkers have been used to deliver drugs without any covalent modifications after cytoplasmic release.

pHLIP has been shown both *in vitro* and *in vivo* to translocate small molecules tethered to the C-term of the peptide. Initial studies showed efficacy in delivering small macrocycles and heterocycles, including taxol and doxorubicin, to cancerous cells. Studies using phalloidin constructs were also able to show successful targeting and delivery to cancer cells. A variety of small molecules have now been shown to be feasible pHLIP cargoes. Additionally, C-term tethering may be used to localize a particular molecule to the intracellular membrane surface. Recent work has expanded this model to include small peptides and potential inhibitors of transmembrane protein dimerization. The use of C-term tethering and delivery is well established in the scientific literature (Thevenin *et al.*, 2009)

The use of pHLIP to localize compounds to the external surface of target cell membranes has not been investigated as heavily as C-term tethered delivery. *In vivo* studies have used N-term tethered fluorophores to image tumors and areas of inflammatory responses with minimal off-target accumulation. Whole-body imaging in rats has shown pHLIP constructs to be stable enough to reach and identify various types of pathology *in vivo* (Andreev *et al.*, 2007). While pHLIP constructs can be cleared from circulation within 24 hours of administration, accumulation in tumors has been observed for over a week (Fendos and Engelman, 2012). Alexa750-pHLIP has shown the ability to preferentially target metastatic lesions, allowing

relative assessment of tumor aggressiveness within a patient. Additionally, Alexa750-pHLIP constructs have been able to identify spontaneous tumours (Reshetnyak *et al.*, 2011). pHLIP constructs have also been used to create novel positron-emission tomography (PET) technology, which capitalizes upon pHLIP insertion to aid in tumor imaging (Vāvere *et al.*, 2009).

The Present Study

A potential use of pHLIP that has yet to be reported in the literature is the use of N-term pHLIP constructs to deliver large, bulky proteins to cancer cell membranes. In the present study, GFP-pHLIP constructs were used as a model system to elucidate the properties of pHLIP-protein constructs. Enhanced green-fluorescent protein (eGFP), a fluorescent protein that has been used as a reporter protein in numerous protein dynamics assays, served as a stand-in for an functionally relevant protein. GFP's fluorescence is dependent upon its proper folding and is pH and temperature dependent. Therefore, disruptions of normal GFP structure caused by pHLIP conjugation or subsequent membrane tethering may manifest as alterations in normal eGFP fluorescence. eGFP excites at 488 nm and emits at a maximal wavelength of 510 nm.

Methods

Preparation of GFP-pHLIP Constructs

An eGFP-containing pET 28a plasmid was engineered to contain a pHLIP peptide sequence following the N-terminus of the eGFP, with a His-tag for purification purposes. Two different H-GFP-pHLIP constructs were prepared; H-GFP-pHLIP, and one with a short glycine-glycine-serine (GGS) linker to allow flexibility between the two portions. The GGS linker was chosen as it is not believed to be recognized by any major family of proteases. GFP-pHLIP constructs were produced via standard *E. coli* protein expression. Briefly, the recombinant pET-28a plasmid with GFP-pHLIP was introduced into *E. coli* cells using standard heatshock

techniques. Recombinant *E. coli* was cultured and grown up; proteins were harvested and target constructs were isolated via nickel-NDA column purification and characterized subsequently via MALDI-TOF mass spectrometry.

Preparation of Silica-Bead Supported Bilayers (SBSBs)

Stock solution of 25 mg/mL 1-palmitoyl,2-oleoyl-sn-glycero-3-phosphocholine (POPC) was dried via vacuum in a desiccator. POPC was solubilized in 5 mM Na₂HPO₄ (pH 8.0) with gentle mixing and heating to a final concentration of 3 mg/mL. Large unilamellar vesicles (LUVs) were converted to small unilamellar vesicles (SUVs) via sonication. The POPC solution was sonicated to clarity using a Branson tip sonicator on ice, pulsed 10s on/off (power level ~3, duty cycle 20%, 30-60 minutes).

Once SUVs had been obtained, they were mixed with monodispersed silica nanoparticles (bath sonicated in Branson 4500 bath sonicator, ~1 minute) and shaken for an hour, with intermittent, gentle vortexing (once every ten minutes). A typical sample consisted of 650 μ L 3 mg/mL SUV solution and 500 μ L 25 mg/mL silica; 6-8 samples were prepared per batch. Total vesicle and particle ratios were calculated to have an A_v/A_p (total vesicle surface area to total particle surface area) ratio of at least 30 (Nordlund *et al.*, 2009). Newly prepared SBSBs were washed twice, with centrifugation (quick tabletop spins, <1 minute), and resuspended in buffer for storage.

To verify protocol success, a carboxyfluorescein-containing POPC lipid sample was used in the synthesis of control SBSBs. Green-field fluorescent microscopy was used to assess the presence of the fluorescent probe on silica microparticles. Images were processed using the ImageJ software.

GFP-pHLIP and SBSB Assays

SBSB aliquots were spun down and resuspended in 200 μ L of 2.5 μ M GFP-pHLIP construct. After an initial 20-min equilibration period at pH 8.0, the pH was lowered to pH 5.0 for 20 minutes. Afterwards, the SBSBs were washed and spun down 3x at pH 5.0, resuspended in 200 μ L buffer, and adjusted to pH 8.0. Fluorescence readings were taken at multiple points during the process: baseline ($t=0$), post-equilibration ($t=20$), after pH adjustment ($t=20$ pH 5.0), after low pH incubation ($t=40$), and after washing, resuspension, and pH neutralization ($t=40$ pH 8.0). Supernatants from each wash were also adjusted to pH 8.0 and assessed as needed. Control samples were treated similarly, though with a constant pH of 8.0. Readings from the control samples were taken at the same relative time points.

Fluorescence was measured using a Cary Eclipse fluorometer, set to emission mode. Samples were excited at $\lambda = 488$ nm and emission spectra obtained from 500-650 nm. Emission maxima were confirmed at 510 nm for all samples; this intensity peak was isolated for further analysis and graphical representation. 5 slits were used for both excitation and emission.

In Vitro Cell Assays

HeLa cells grown in DMEM complete media were seeded in 4-well glass plates approximately 48 hours prior treatment and allowed to grown to confluence. Once cells were ready for treatment, growth media was removed and treatment applied. Treatment consisted of a 30 minute incubation of the construct diluted in media. After treatment had been completed, cells were washed 3x rapidly, bathed in recovery media (DMEM complete), and assessed under a fluorescence-enabled microscope. Initially, 5 and 10 μ M GFP-pHLIP were used at pH 6.0 and pH 7.4; after confirming the feasibility higher concentrations in these assays, 10 μ M construct was used exclusively. DMEM buffered with bicarbonate was used in the pH 7.4 treatment, while DMEM buffered with citric acid was used at pH 6.0.

Images were taken using a Nikon camera attachment. Photographs were initially taken using auto-exposure settings; subsequent imaging used this exposure period to ensure consistency across images. Optical (brightfield) and fluorescent (green-field) images were taken of each sample at various locations to allow comparison of cell location and fluorescence localization. Images were processed using the ImageJ software.

Results

Verification of Supported Bilayer Synthesis

Imaging of carboxyfluorescein-containing POPC lipid bilayers confirmed the successful synthesis of SBSBs. Bright field imaging clearly identified the location of beads, while follow-up fluorescent imaging showed a distinct localization of fluorescent signal to the beads. This confirms that SUVs collapsed onto the silica beads to create supported bilayers.

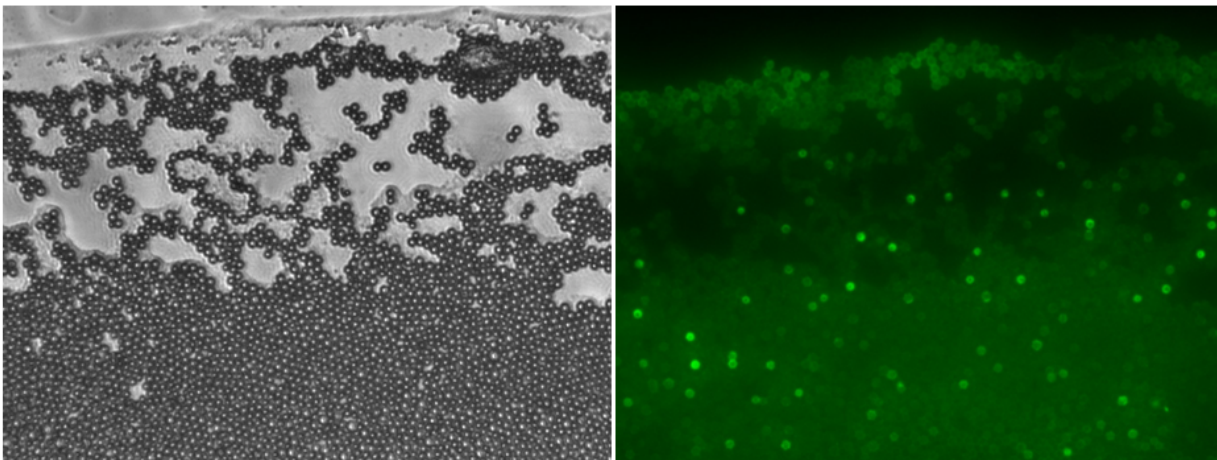


Figure 1. Bright field image showing silica microparticles (*left*). Green-field fluorescent capture confirms presence of carboxyfluorescein tag on silica nanoparticles, indicating bilayers are collapsed upon beads (*right*). Fluorescent image was pseudocolored in ImageJ.

SBSB Assays

In several of the assays, initial fluorescence declined dramatically before reaching a time-stable baseline (data not shown). As a general trend, fluorescence declined dramatically after lowering of pH with minimal recovery after readjustment to pH 8. Control samples did not show

major loss of signal post-washing, contrary to the hypothesized results. One set of experiments, however, stand as an exception to these general trends.

In one trial, the hypothesized behavior of GFP-pHLIP was observed: GFP-pHLIP was retained upon low pH treatment, while controls showed a nearly complete loss of signal upon washing, with GFP-pHLIP presence detected in the supernatants. Fluorescence recovery of the experimental sample was also observed in this trial, though the intensity is less than 20% of its original value, even upon prolonged incubation at physiological pH. The lost fluorescence was not detected in the supernatants obtained after washing, even after incubation at pH 8 for over 20 minutes. The results of this experiment are shown graphically in Figure 2. Emission maxima values at $\lambda = 510$ nm are shown to allow facile comparison of readings.

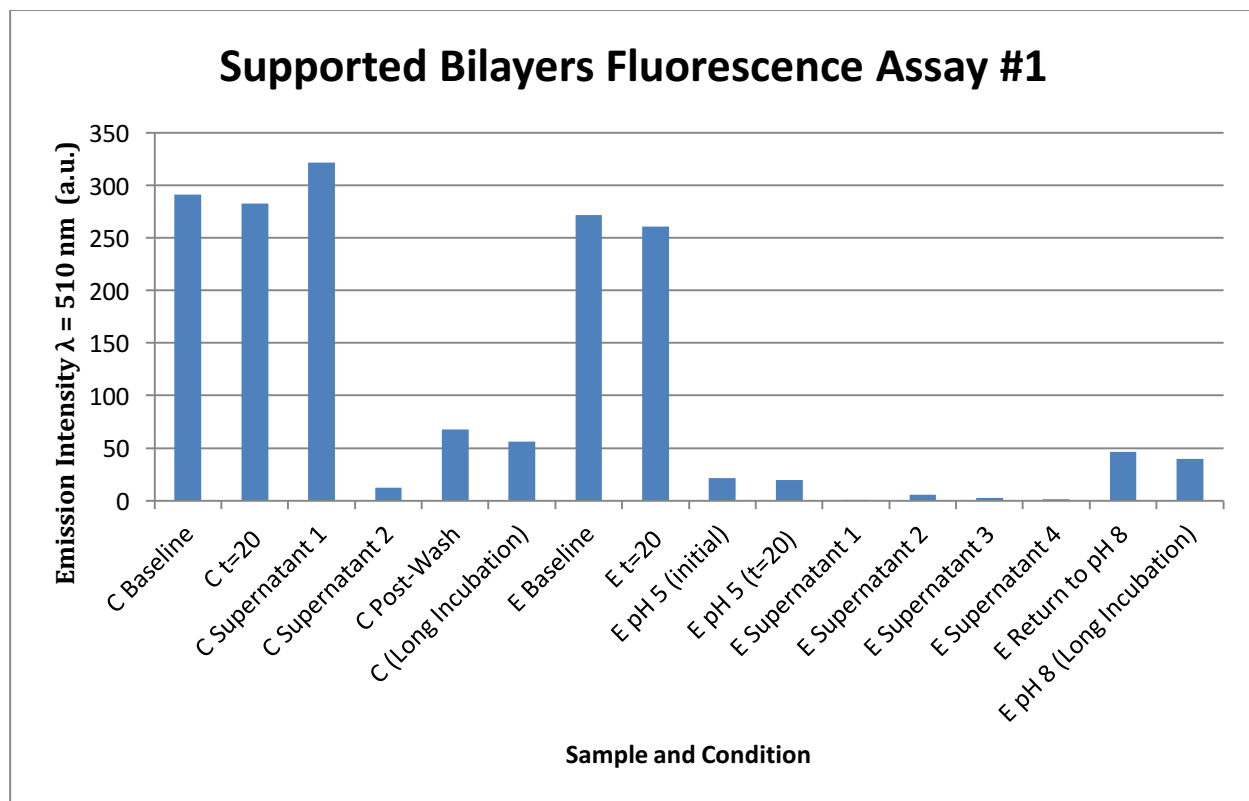


Figure 2. Results of an initial SBSB GFP-pHLIP fluorescence assay. C denotes the control sample, while E denotes the experimental sample (subjected to pH adjustments). Emission values at $\lambda = 510$ nm, the maxima of eGFP, are shown along the y-axis. Low pH treatment led to retention of GFP-pHLIP, though the signal was greatly reduced, while the construct washed out of control samples.

The results of a representative GFP-pHLIP characterization assay using SBSBs are shown in Figure 3. The control sample showed a fairly consistent fluorescence, with moderate decline post-washing. The experimental sample showed a pH-dependent decline in fluorescence, but did not show a significant recovery after pH readjustment. The lost signal was not present in supernatants, pointing to a lasting effect of lowered pH on sample structure in the presence of SBSBs. It is also important to note the low fluorescence values, in general, compared to the free construct and the specific trial reported previously in this paper. It is unknown why fluorescence values were so highly variable across experiments.

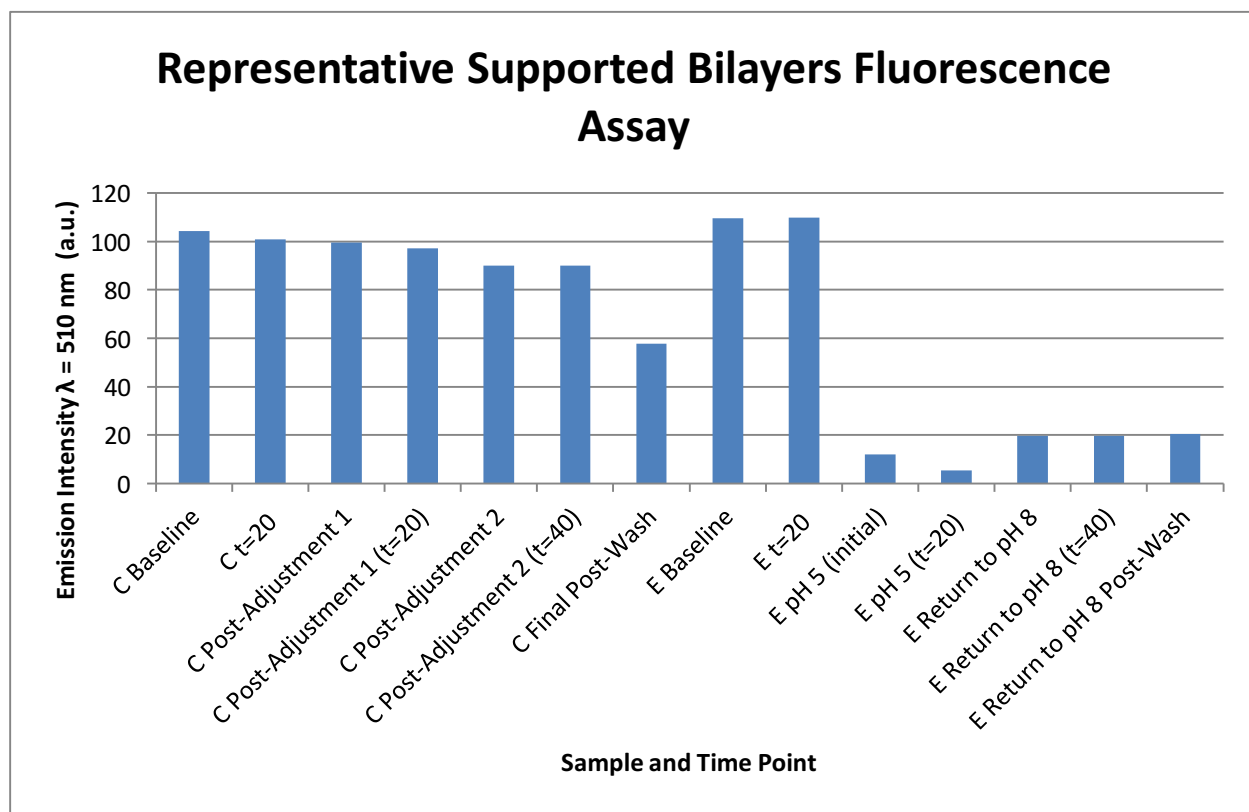


Figure 3. Results of a representative SBSB fluorescence assay. After pH adjustment, there is a noticeable loss of signal. Upon pH readjustment, there is a slight return of fluorescence. It is important to note that, in the control condition, there is only a moderate loss of signal after washing and centrifugation.

In Vitro Cell Assays

Results of HeLa cell culture assays were promising. Brightfield microscopy confirmed location of cells, while fluorescent microscopy confirmed GFP-pHLIP presence in the vicinity of cells. Sample fluorescence was clearly visible in all conditions. Compared to control cells, those treated at pH 6.0 showed greater levels of fluorescence after washing. The enhanced fluorescence was observed in distinct spots of brightness. Cell distribution appeared consistent throughout the four wells, though initial studies showed what appeared to be construct aggregation peripherally in each well. This may have been due to culture quality, as later experiments using healthier and more confluent cells did not yield suspected peripheral construct aggregation.

Given the nature of fluorescence microscopy, we are unable to determine the exact location of fluorescent signals relative to cell membranes or the nature of clustering. A moderate clumping of cells was observed at later times during imaging, likely a result of cells leaving optimal culture conditions during imaging. This effect was captured in several images (data not shown).

Figure 4 shows images of HeLa cells treated with GFP-pHLIP. Fluorescent images were not quantitatively analyzed. Enhanced fluorescent signal, represented by green pseudocoloring, is indicative of membrane insertion and resultant retention of construct post-washing.

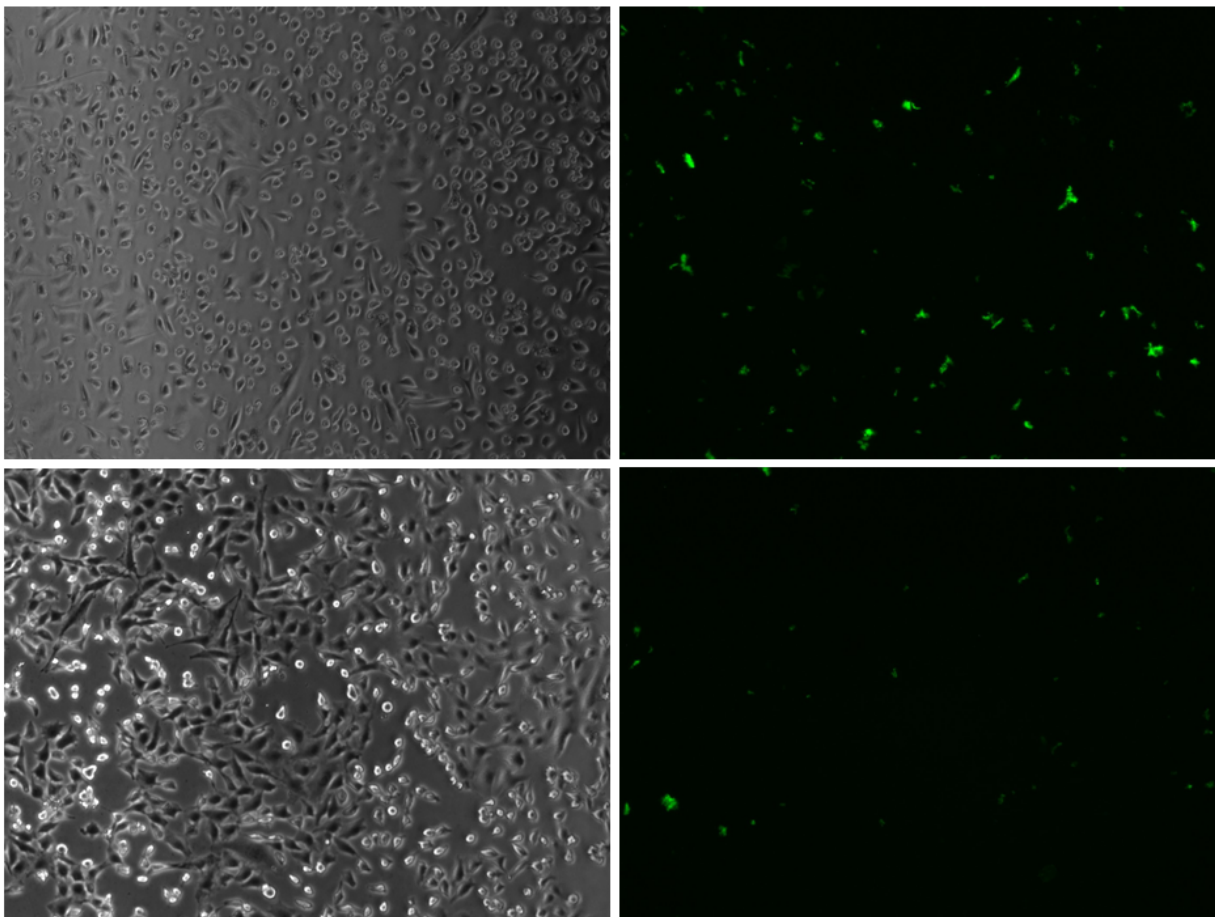


Figure 4. Captured images of GFP-pHLIP in HeLa cell assays. Top images are of cells treated with GFP-pHLIP at pH 6.0; bottom images are of control cells (treated at pH 7.4). Brightfield imaging (*left*) verifies the presence of cells. Green-field fluorescent imaging (*right*) shows a distinct difference between the two conditions, with enhanced signal obtained from the low pH treatment. Fluorescent images pseudocolored in ImageJ.

Discussion

The use of pHLIP as a targeting system to deliver proteins selectively to cancer cell membranes requires further study to validate. In the present studies, preliminary data suggests a degree of selectivity of membrane insertion and maintenance of pHLIP properties when linked to GFP, a larger, bulkier cargo than has been reported before. *In vitro* studies in HeLa cultures show clustering and what appears to be localization to cell membranes, effects enhanced by lowering the pH. Similarly, *in vitro* studies using supported bilayers show a slight increase in membrane insertion at lower pH. The data, however, do not conclusively show a pH-dependent insertion of GFP-pHLIP without loss of function of either constituent.

The supported bilayer studies require further elaboration to conclusively show pH dependent insertion of GFP-pHLIP. As it currently stands, GFP fluorescence is our sole indicator of enhanced membrane insertion. There are two major limiting factors that arise given this constraint. First, the presence of GFP makes impossible the use of CD and oriented CD, traditionally used to confirm pHLIP transition to a helical state. Thus, given the presence of GFP fluorescence post-washing in most trials, it is difficult to discern whether pHLIP insertion or simple bilayer interactions and aggregation are responsible for the increased pHLIP retention in lower pH conditions.

The second factor is a difficulty in recovering baseline GFP fluorescence after low pH treatment. Control studies of free GFP-pHLIP in standard buffers showed a quick, clear transition in fluorescence intensity in the range of pH 6: below pH 6, fluorescence was virtually absent, while at physiological pH, fluorescence was clear and intense. However, similar studies performed in the presence of supported bilayers (essentially the assay without washing and centrifugation steps), were unable to replicate this recovery. When recovery was observed, emission intensity peaked at roughly 20% of the baseline values. Prolonged incubation at higher pHs did not significantly enhance fluorescence recovery, pointing to a lasting loss of structure upon pH adjustment. A requirement of our assay design is the recovery of GFP fluorescence after returning to physiological pH. Thus, if GFP-pHLIP fails to properly refold after low-pH treatment, even if it has inserted into membranes in a pH-dependent fashion, we would be unable to detect its presence or retention in membranes.

A lurking variable may be the particular supported bilayers used in the study. While most studies use silica nanoparticles with diameters in the 100-600 nm range, the beads used here were significantly larger (3 μm). Thus, while full bead coating was confirmed in earlier stages

using fluorescent lipid tags, it may have followed that subsequent preps did not successfully synthesize uniformly coated beads.

To expand on the present work, there are several factors that can be modulated. The use of smaller beads, preferably in the 600 nm diameter range, would greatly increase the surface-area-to-volume ratio of supported bilayers, allowing the use higher concentrations of protein construct without the risk of overloading bilayer surfaces. This change would also further align the given studies with previous work reported in the literature investigating protein and supported bilayer interactions.

The assays of GFP-pHLIP in cell culture appear to be more promising, as a noticeable increase in fluorescent signal was seen in lower pH conditions. Further studies are needed to address two concerns, which may be related: the presence of a significant baseline signal in control conditions (in which minimal pHLIP insertion should be observed) and the possibility of pH-induced construct aggregation. The use of confocal microscopy would allow both issues to be addressed; confirming the membrane to be the site of fluorescence would provide evidence pHLIP insertion is the reason for enhanced construct retention at lower pHs.

While the assays performed in cell culture yielded promising results, cell viability was of concern. As the imaging process continued and cells remained outside their preferred incubation conditions, clustering and clumping was observed. Cells that react unfavorably to changing conditions may very well interfere with concurrent imaging and skew the obtained results. Therefore, the use of fixed cells in similar studies is a potential next step. Alternatively, analyzing the insertion of GFP-pHLIP via flow cytometry may aid in confirming pHLIP insertion in target membranes.

One cause for concern in both assays, which may point to construct aggregation and *not* membrane insertion as the cause of increased retention at low pH, is the presence of a moderate signal in the control conditions. At pH 8.0, pHLIP membrane insertion should be minimal, below the threshold needed to see the amount of signal observed in control conditions. As such, further characterization of the GFP-pHLIP constructs is needed. During sample preparation, it was also noticed that constructs were difficult to solubilize, and in some cases, may have been aggregating at the concentrations used; this was noted to be unusual, as pHLIP constructs are typically soluble well above the concentrations used in the present study.

Given the difficulties in solubilizing the constructs initially and the propensity for pHLIP conjugates to aggregate in abnormal conditions, it may be the case that GFP-pHLIP is aggregating, either with itself or in association with supported bilayers. Such aggregates, if tethered strongly enough to supported bilayers, would be retained even through washing and centrifugation. These aggregates, even in the prolonged presence of heightened pH, would be less likely to dissociate and refold to their native states, hampering fluorescence recovery.

Dialysis of prepared constructs appeared to aid solubility; further studies using processed constructs may be able to address the aggregation issues noted here. If aggregation is eliminated and the baseline retention rates of GFP-pHLIP drop significantly, concerns of nonselective targeting can be allayed.

Once GFP-pHLIP has been established as a model for pHLIP-mediated protein delivery to cell membranes, pHLIP-enzyme constructs would be the logical next step in the development of this technique. One could envision a construct in which an enzyme that is deficient in cancerous tissue is localized via pHLIP to the cell's external microenvironment, possibly facilitating production of a compound that would slow the tumor's growth. Another scheme

would use the localized enzyme to locally cleave a systemically administered pro-drug to its active form in select locales. Immune adjuvants, such as key regulators of the complement system, may also be of interest.

References

- Andreev OA, Dupuy AD, Segala M, Sandugu S, Serra DA, Chichester CO, Engelman DM, Reshetnyak YK (2007). Mechanism and uses of a membrane peptide that targets tumors and other acidic tissues in vivo. *Proc Natl Acad Sci.* 104(19):7893-7898.
- Barar J, Omid Y (2013). Dysregulated pH in Tumor Microenvironment Checkmates Cancer Therapy. *BioImpacts.* 3(4):149-162. doi: 10.5681/bi.2013.036
- Barrera FN, Weerakkody D, Anderson M, Andreev OA, Reshetnyak YK, Engelman DM (2011). Roles of carboxyl groups in the transmembrane insertion of peptides. *J Mol Bio.* 413(2):359-371. doi: 10.1016/j.jmb.2011.08.010.
- Fendos G, Engelman D (2012). pHLIP and acidity as a universal biomarker for cancer. *Yale J Biol Med.* 85(1):29-35
- Gatenby RA, Gillies RJ (2004). Why do cancers have high aerobic glycolysis? *Nat Rev Cancer.* 4(11):891-899.
- Haddley K (2012). Brentuximab vedotin: its role in the treatment of anaplastic large cell and Hodgkin's lymphoma. *Drugs Today (Barcelona)* . 48:259–270.
- Hunt JF, Earnest TN, Bousché O, Kalghatgi K, Reilly K, Horváth C, Rothschild KJ, Engelman DM (1997a). A biophysical study of integral membrane protein folding. *Biochemistry.* 36(49):15156-15176.
- Hunt JF, Rath P, Rothschild KJ, Engelman DM (1997b). Spontaneous, pH-dependent membrane insertion of a transbilayer alpha-helix. *Biochemistry.* 36(49):15177-15192.
- Jang M, Kim SS, Lee J (2013). Cancer cell metabolism: implications for therapeutic targets. *Experimental & Molecular Medicine.* e45:1-8. doi:10.1038/emm.2013.85

- LoRusso PM, Weiss D, Guardino E, Girish S, Sliwkowski MX (2011). Trastuzumab emtansine: a unique antibody drug conjugate in development for human epidermal growth factor receptor 2-positive cancer. *Clin. Cancer Res.* 17:6437-6447.
- Musial-Siwiek M, Karabadzhak A, Andreev OA, Reshetnyak YK, Engelman DM (2010). Tuning the insertion properties of pHLIP. *Biochim Biophys Acta.* 1798(6):1041-1046. doi: 10.1016/j.bbamem.2009.08.023
- Nordlund G, Lönneborg R, Brzezinski P (2009). Formation of supported lipid bilayers on silica particles studied using flow cytometry. *Langmuir.* 25(8):4601-4606. doi: 10.1021/la8036296.
- Reshetnyak YK, Andreev OA, Lehnert U, Engelman DM (2006). Translocation of molecules into cells by pH-dependent insertion of a transmembrane helix. *Proc Nat Acad Sci.* 103(17):6460-6465.
- Reshetnyak YK, Segala M, Andreev OA, Engelman DM (2007). A monomeric membrane peptide that lives in three worlds: in solution, attached to, and inserted across lipid bilayers. *Biophys J.* 93(7):2363-2372.
- Reshetnyak YK, Yao L, Zheng S, Kuznetsov S, Engelman DM, Andreev OA (2011). Measuring tumor aggressiveness and targeting metastatic lesions with fluorescent pHLIP. *Mol Imaging Bio.* 13(6):1146-1156. doi: 10.1007/s11307-010-0457-z.
- Thévenin D, An M, Engelman DM (2009). pHLIP-mediated translocation of membrane-impermeable molecules into cells. *Chem Biol.* 16(7):754-62. doi: 10.1016/j.chembiol.2009.06.006.
- Tomlinson IPM, Novellie MR, Bodmer WF (1996). The mutation rate and cancer. *Proc Natl Acad Sci.* 93: 14800–14803

Vāvere AL, Biddlecombe GB, Spees WM, Garbow JR, Wijesinghe D, Andreev OA, Engelman DM, Reshetnyak YK, Lewis JS (2009). A novel technology for the imaging of acidic prostate tumors by positron emission tomography. *Cancer Res.* 69(10):4510-4516. doi:10.1158/0008-5472.